Tissue and Cell xxx (2016) xxx–xxx

Contents lists available at ScienceDirect

Tissue and Cell

journal homepage: www.elsevier.com/locate/tice

SPCA2 couples Ca^{2+} influx via Orai1 to Ca^{2+} uptake into the Golgi/secretory pathway

Susanne Smaardijk, Jialin Chen, Frank Wuytack, Peter Vangheluwe*

Laboratory of Cellular Transport Systems, Department of Cellular and Molecular Medicine, KU Leuven, Leuven, Belgium

ARTICLE INFO

Article history:
Received 4 May 2016
Received in revised form 29 July 2016
Accepted 2 September 2016
Available online xxx

Keywords:
Orai1
Store independent Ca^{2+} entry
Store dependent Ca^{2+} entry
Ca^{2+} Transport
Lactation
Breast cancer
Golgi
Secretory pathway

ABSTRACT

Dysregulation of the Golgi/Secretory Pathway Ca^{2+} transport ATPase SPCA2 is implicated in breast cancer. During lactation and in luminal breast cancer types, SPCA2 interacts with the plasma membrane Ca^{2+} channel Orai1, promoting constitutive Ca^{2+} influx, which is termed store independent Ca^{2+} entry (SICE). The mechanism of SPCA2/Orai1 interaction depends on the N- and C-termini of SPCA2. These extensions may play a dual role in activating not only Orai1, but also Ca^{2+} transport into the Golgi/secretory pathway, which we tested by investigating the impact of various SPCA2 N- and/or C-terminal truncations on SICE and Ca^{2+} transport activity of SPCA2. C-terminal truncations impair SICE and SPCA2 activity, but also affect targeting, whereas N-terminal truncations affect targeting and inactivate SPCA2, but remarkably, SICE activation remains unaffected. Importantly, overexpression of SPCA2 increases the Ca^{2+} content of non-ER stores, which depends on Orai1 and SPCA2 activity. Thus, Orai1-mediated Ca^{2+}-influx and SPCA2-mediated Ca^{2+} uptake activity into the Golgi/secretory pathway might be coupled possibly in a microdomain. This channel/pump complex may efficiently transfer Ca^{2+} into the secretory pathway, which might play a role in SPCA2-expressing secretory cells, such as mammary gland during lactation.

1. Introduction

Ca^{2+} is an important second messenger that is implicated in a variety of cellular processes, including secretion, muscle contraction, cell division and apoptosis (Berridge et al., 2003). The Golgi Apparatus participates in shaping the spatiotemporal regulation of Ca^{2+} storage and cytosolic Ca^{2+} signaling in the cell (Pizzo et al., 2011; Rizzuto and Pozzan, 2006; Vanoevelen et al., 2005b). The concentration of Ca^{2+} in the Golgi Apparatus is heterogeneous, ranging between 250 μM in the *cis*-Golgi to 130 μM in the *trans*-Golgi (Pizzo et al., 2010). The high luminal Ca^{2+} concentration promotes protein folding and is needed for enzymatic activities such as glycosylation (Durr et al., 1998; Vangheluwe et al., 2009). The Golgi Apparatus also contributes to Ca^{2+} signaling by releasing Ca^{2+} via inositol-1,4,5-triphosphate receptors or ryanodine receptors in the Golgi (Wong et al., 2013). Finally, local Ca^{2+} uptake in the *trans*-Golgi network organizes luminal protein sorting possibly leading to recruitment of Ca^{2+} binding proteins into budding vesicles for transport (Kienzle et al., 2014; von Blume et al., 2011).

Two Ca^{2+} pumps control Ca^{2+} uptake into the Golgi: the sarco/endoplasmic reticulum Ca^{2+} transport ATPase SERCA2b, which is mainly found in the endoplasmic reticulum (ER), but also in the *cis*-Golgi, and the more abundant secretory pathway Ca^{2+}/Mn^{2+} transport ATPase SPCA, which is detected throughout the Golgi Apparatus and in secretory vesicles. These closely related Ca^{2+} transport ATPases undergo a reaction cycle that involves two major conformational states: E1 with high Ca^{2+} affinity binding sites facing the cytosol, and E2 with low Ca^{2+} affinity binding sites facing the lumen. During transport, the pumps undergo transient autophosphorylation at a conserved aspartate residue, which controls access to the Ca^{2+} binding sites (Moller et al., 2005).

Two SPCA isoforms exist in humans: the ubiquitous Ca^{2+} pump SPCA1, and SPCA2, which displays a more restricted expression pattern limited mainly to secretory cells in mammary epithelia, the gastrointestinal tract and testes (Vanoevelen et al., 2005a; Xiang et al., 2005). SPCA1 primarily fulfills a housekeeping function to provide the Golgi with Ca^{2+} and Mn^{2+}, although SPCA1 is also involved in Mn^{2+} detoxification in the liver (Leitch et al., 2011). Heterozygous mutations in human SPCA1 give rise to Hailey–Hailey disease, an autosomal dominant skin disease that is characterized by acantholysis and dyskeratosis (Sudbrak et al., 2000), whereas mouse *Atp2c1* null mutants are embryonically lethal by failure of neural tube closure (Okunade et al., 2007). The predominant expression of SPCA2 in secretory cell types suggest a role of SPCA2 in secretion (Vanoevelen et al., 2005a; Xiang et al., 2005).

* Corresponding author at: Laboratory of Cellular Transport Systems, Department of Cellular and Molecular Medicine, KU Leuven Campus Gasthuisberg, Herestraat 49, Box 802, B3000 Leuven, Belgium.
E-mail address: peter.vangheluwe@kuleuven.be (P. Vangheluwe).

http://dx.doi.org/10.1016/j.tice.2016.09.004
0040-8166/

In lactating mammary gland, SPCA1 and SPCA2 are highly upregulated and promote Ca^{2+} into the Golgi/secretory pathway supporting *trans*-epithelial Ca^{2+} transport, which accounts for 40% of the Ca^{2+} release into the milk (Faddy et al., 2008; Reinhardt et al., 2000; Reinhardt et al., 2004). Of interest, SPCA2, but not SPCA1, directly interacts with and activates the Ca^{2+} channel Orai1, the plasma membrane (PM) constituent of Ca^{2+}-release activated Ca^{2+} (CRAC) channels, which in mammary gland may potentiate cellular Ca^{2+} uptake for release into the milk (Feng et al., 2010). Within the PM, the N-terminus of SPCA2 first binds to Orai1, thereby enabling the much shorter C-terminus to come close enough to interact and subsequently activate the CRAC channel. This process is termed Store-Independent Ca^{2+} Entry (SICE), since it occurs independent of ER Ca^{2+} depletion and relocalization of STIM1 (Feng et al., 2010). This is different from Store-Operated Ca^{2+} entry (SOCE), the 'classical' mechanism of activation of CRAC channels by STIM1 in conditions of reduced ER Ca^{2+} levels (Park et al., 2009; Zhang et al., 2005).

Orai1, SPCA1 and SPCA2 are implicated in breast cancer. Orai1 expression is elevated in basal-type tumor samples and in mammary tumor cell lines, including MCF-7 and MDA-MB-231 (McAndrew et al., 2011). In basal-like breast cancer cell lines, including MDA-MB-231 cells, SPCA1 is elevated (Dang and Rao, 2016; Feng et al., 2010; Grice et al., 2010) and inhibition of SPCA1 may be considered as a therapeutic strategy, since in MDA-MB-231 cells this impairs the processing of the insulin-like growth factor receptor, which is involved in tumor progression (Grice et al., 2010). SPCA2 expression is upregulated in luminal-type breast cancer types (Faddy et al., 2008). In MCF-7 cells, SPCA2 physically interacts with Orai1 leading to a constitutive Ca^{2+} influx that stimulates proliferation (Feng et al., 2010). Indeed, knockdown of either SPCA2 or Orai1 in MCF-7 cells attenuates cell proliferation, colony formation in soft agar and tumor formation in nude mice, whereas SPCA2 overexpression in non-tumorigenic MCF-10A cells promotes colony formation in soft agar (Feng et al., 2010). Thus, the SPCA2/Orai1 dysregulation leads to a pathological Ca^{2+} influx that contributes to the proliferative nature and tumorigenic potential of these breast cancer cell types.

In this paper, we confirm and further extend insights into the interaction between SPCA2 and Orai1 by the N- and C-termini of SPCA2. Since isoform specific N- and C-terminal extensions of Ca^{2+} transport ATPases often exert signaling/scaffolding functions, which are coupled to the regulation of Ca^{2+} transport (Falchetto et al., 1992; Gorski et al., 2012), we hypothesized that N- and C-terminal stretches of SPCA2 might exert a dual function stimulating Ca^{2+} influx via Orai1, while promoting Ca^{2+} uptake into the Golgi/secretory pathway. To explore this, we generated a series of N- and C-terminally truncated constructs of SPCA2, which were tested for their subcellular localization, auto-phosphorylation activity, intracellular Ca^{2+} uptake and stimulation of SICE.

2. Materials and methods

2.1. DNA, cell culture and transfection

Human SPCA1a and SPCA2 cDNA was inserted into pcDNA6 destination vectors (Gateway®) with or without an N-terminal mCherry- or GFP-tag. N-terminal mCherry-SERCA2b and mCherry-STIM1 constructs were used (Baron et al., 2010). Mutants were generated using the Quickchange® site-directed mutagenesis kit (Stratagene). HEK293T cells were cultured at 37 °C and 10% CO_2. HeLaT1 and COS cells were cultured at 37 °C and 5% CO_2. Cells were kept in Dulbecco's Modified Eagle Medium supplemented with 10% fetal bovine serum, 100 IU/ml penicillin, 100 mg/ml streptomycin, 2 mM Glutamax (Thermo Fisher Scientific) and non-essential amino acids (Thermo Fisher Scientific, only for HEK293T and COS cells). GeneJuice transfection reagent (Thermo Fisher Scientific) was used for transfection according to the manufacturer's instructions. Cotransfection of plasmid DNA and siRNA oligos (OnTarget Plus SMART pool, Dharmacon) was achieved with Dharmafect Duo (GE Life Science). The siRNA used was a mixture of the following target sequences: non-targeting siRNA: UGGUUUACAUGUCGACUAA, UGGUUUACAUGUUGUGUGA, UGGUUUACAUGUUUUCUGA, UGGUUUACAUGUUUUCCUA; Orai1 siRNA: UCAACGAGCACUCCAUGCA, GGAGUUUGCCCGCUUACAG, GCACCUGUUUGCGCUCAUG, GGCCUGAUCUUUAUCGUCU.

2.2. Fluorescence imaging and NFAT translocation

HEK293T cells or HeLaT1 cells were seeded at 15,000 cells/well in chamber slides (NUNC) and transfected with 300 ng DNA. 72 h after transfection, cells were fixed with 4% paraformaldehyde (Sigma-Aldrich) prior to fluorescence microscopy. For NFAT-GFP translocation, cells were co-transfected with SPCA1a or SPCA2 and NFAT-GFP in a 5:1 ratio. We verified via immunostaining with an SPCA antibody that a similar percentage of cells was transfected with the different SPCA constructs. Per condition, a minimum of 100 cells was compared to determine the percentage of cells with nuclear NFAT translocation. For TGN staining, cells were fixed with 4% paraformaldehyde, permeabilized with 0.2% Triton X-100, incubated for 1 h with anti-TGN46 (Thermo Scientific, 1:500) and 1 h with Alexa Fluo 488 anti-rabbit (Fischer Scientific, 1:2000). Visualization was performed on an Olympus IX81 fluorescence microscope with excitation/emission wavelengths 469/510 nm (GFP) or 562/610 nm (mCherry).

2.3. Fura2-AM intracellular Ca^{2+} measurements

For Ca^{2+} imaging, HEK293T cells were transfected with mCherry-tagged SPCA constructs. The procedure was carried out as described in Vervliet et al. (2014). 72 h after transfection, cells were incubated for 30 min in a modified KREBS solution (11.5 mM glucose, 1.5 mM $CaCl_2$, 135 mM NaCl, 6.2 mM KCl, 1.2 mM $MgCl_2$, 12 mM HEPES, pH 7.3) supplemented with 1 μM Fura2-AM (Life Sciences), and subsequently washed for 30 min in the same modified KREBS solution. mCherry-positive cells with comparable fluorescence intensity were selected and visualized at room temperature at excitation wavelengths of 340 and 380 nm and emission wavelength 510 nm on a Zeiss Axio Observer Z1 Inverted Microscope. Extracellular Ca^{2+} was depleted by adding modified KREBS supplemented with 3 mM BAPTA (Alfa Aesar) to the cells. Ca^{2+} release from ER and non-ER stores was assessed by adding respectively 500 nM thapsigargin (Alomone labs) or 2 μM ionomycin (Enzo Life Sciences) in modified KREBS supplemented with 3 mM BAPTA. CRAC channels were inhibited by 10 μM 3,5-bistrifluoromethyl pyrazole (YM-58483/BTP2, Abcam), which was added in modified KREBS (Zitt et al., 2004).

2.4. Total membrane preparation and immunoblotting

4.1 million HEK293T cells were seeded per 15 cm petri dish one day prior to transfection. For MG-132 treatment, cells were incubated for 6 h with 10 μM MG-132 (Sigma-Aldrich) prior to homogenization. Membrane preparation was carried out as described in Sepúlveda et al. (2008). 72 h after transfection, HEK293T cells were homogenized in homogenization buffer (10 mM HEPES pH 7.4, 0.32 M sucrose, 0.5 mM $MgSO_4$, 0.1 mM phenylmethanesulfonyl fluoride, 2 mM β-mercaptoethanol, 1× Sigmafast protease inhibitor (Sigma-Aldrich)) and centrifuged at 1,500*g* for 10 min. The supernatant was centrifuged at 100,000*g* for 45 min to collect the total membrane fraction. The pellet was

Please cite this article in press as: Smaardijk, S., et al., SPCA2 couples Ca^{2+} influx via Orai1 to Ca^{2+} uptake into the Golgi/secretory pathway. Tissue Cell (2016), http://dx.doi.org/10.1016/j.tice.2016.09.004

dissolved in 0.25 M sucrose and protein concentration was determined via the Qubit method (Life Sciences). To compare the relative SPCA2 expression levels, 10 μg protein was loaded on a 4–12% Bis-Tris gel (NuPAGE, Thermo Scientific). Gel electrophoresis was conducted and immunoblotting was performed as described earlier (Vandecaetsbeek et al., 2009). Anti-mCherry (Abcam, 1:5000), anti-GAPDH (Sigma Aldrich, 1:5000) and home-made anti-SPCA2 (XIB, 1:2000; raised against the first cytosolic loop (Vanoevelen et al., 2005a)) antibodies were used, followed by a secondary HRP labeled anti-rabbit or anti-mouse antibody incubation (1:2000, Bioke). Visualization was performed with an enhanced chemiluminesence detection kit (Pierce) on a Chemidoc MP (Biorad).

2.5. Auto-phosphorylation assay

The auto-phosphorylation reaction was carried out as described earlier (Holemans et al., 2015). 20 μg protein from the total membrane fractions of COS cells was incubated on ice in 50 μl reaction buffer containing 17 mM HEPES pH 7.0, 160 mM KCl, 1 mM dithiothreitol (DTT) and 2.5 mM NaN_3, supplemented with 1 mM EGTA or 100 μM $CaCl_2$. The auto-phosphorylation reaction was initiated with 5 μl of a mixture containing 5 μM ATP and 25 nM radio-actively labeled γ-^{32}P-ATP. After 20 s, the reaction was stopped by addition of 300 μl stop solution (6% trichloroacetic acid, 10 mM phosphoric acid) and the protein was allowed to precipitate for 30 min on ice. Samples were centrifuged for 15 min at 14,000*g* and the pellet was washed twice with 400 μl stop solution and finally dissolved in 20 μl loading buffer (150 mM Tris-HCl, 8 mM Na-EDTA, 3% sodium dodecyl sulfate (SDS), 20% sucrose, 0.14 mg/ml bromophenol blue, 10 mM DTT, pH 7.4). Proteins were separated via electrophoresis (4 h, 200 V) on an acidic gel (25% acrylamide/bisacrylamide 37.5:1, 64.5 mM Tris-phosphate, 1% SDS, 0.075% ammonium persulfate, 0.075% tetramethylethylenediamine, pH 6.8) in MOPS running buffer (170 mM MOPS, 0.1% SDS, pH 6.3). Gels were dried overnight and exposed to a phosphorscreen for 24 h and analyzed with a Storm840 imager. The intensity of the bands was quantified with ImageJ software.

2.6. Statistics

Origin 8.6 was used for data analysis. Results are presented as average ± SEM. Multiple comparison statistical analysis was carried out by one-way ANOVA followed by a posthoc Fisher test. $P < 0.05$ was considered statistically significant.

3. Results

3.1. SPCA2 triggers SICE independent of its transport function

To set up the protocol of SPCA2 mediated Ca^{2+} entry, we first confirmed findings of Feng et al. (2010) by showing that in HEK293T cells, which do not endogenously express SPCA2, the overexpression of SPCA2, but not SPCA1a, leads to the translocation of the transcription factor NFAT to the nucleus (Fig. 1A and C). NFAT translocation depends on dephosphorylation by calcineurin that is activated by a rise in cytosolic Ca^{2+} ($[Ca^{2+}]_{cyt}$) (Hogan et al., 2003). Via Fura2 Ca^{2+} imaging, we indeed observed that compared to mCherry overexpression, overexpression of mCherry-tagged SPCA2 raises the 340/380 ratio, which is indicative for a higher $[Ca^{2+}]_{cyt}$. Addition of 3 mM BAPTA depletes Ca^{2+} in the extracellular medium and prevents Ca^{2+} influx. This treatment immediately reduces the 340/380 ratio in SPCA2 overexpressing cells to the level of the mCherry control cells (Fig. 1D), which indicates that Ca^{2+} influx was constitutively activated by SPCA2 overexpression. The constitutive Ca^{2+} influx was quantified by determining the R_0/R_{120} value, which is the starting 340/380 ratio at 0 s (R_0) normalized to the 340/380 ratio after addition of BAPTA at 120 s (R_{120}). The R_0/R_{120} in cells overexpressing SPCA2 (1.31 ± 0.036) is significantly higher than the R_0/R_{120} ratio in mCherry control cells (1.03 ± 0.007) (Fig. 1E). Constitutive Ca^{2+} influx can be blocked by addition of BAPTA or the CRAC channel inhibitor BTP2 (Fig. 1F) (Zitt et al., 2004), suggesting that SPCA2 mediates Ca^{2+} influx via Orai1. Importantly, the Orai1 activation seems to occur independent of STIM1, since relocalization of STIM1-mCherry into punctae was not observed (Fig. 1B). As a positive control for SOCE activation in SPCA2 overexpressing cells, 1 μM thapsigargin was supplied to deplete ER Ca^{2+} stores, which promotes STIM1 relocalization (Fig. 1B). This shows that SOCE (STIM1/Orai1) appears to work independently of SICE (SPCA2/Orai1).

Since binding of the SPCA2 N-terminus to Orai1 promotes the access of the SPCA2 C-terminus to allow Orai1 activation (Feng et al., 2010), we hypothesized that the availability of the N- and C-termini for Orai1 interaction/activation might depend on the conformational state of SPCA2, which varies the most between the E1 and E2 states. We therefore aimed to trap SPCA2 predominantly in the E1 state by mutating the site of auto-phosphorylation (D379N), or in the E2P state by mutating the residue that catalyzes the dephosphorylation reaction (E222Q). Compared to wildtype (WT) SPCA2, both mutants are able to induce translocation of NFAT-GFP to the nucleus (Fig. 1C) and lead to a similar increase in constitutive Ca^{2+} influx (Fig. 1D and E). This suggests that the SPCA2/Orai1 interaction may occur in various conformational states of SPCA2 and is able to take place independently of the Ca^{2+} transport activity, which is in line with previous observations (Feng et al., 2010).

3.2. N-/C-truncations lead to mis-targeting, while SICE is impaired by C-terminal deletion only

Next, we investigated a total of six N- or C-terminal truncations of SPCA2 to explore how the N- and C-termini of SPCA2 control Orai1 and SPCA2 transport activity. Truncation sites were chosen based on the SPCA2 secondary structure predicted by iTasser (http://zhanglab.ccmb.med.umich.edu/I-TASSER/, (Zhang, 2008)), and on previously published information on the putative Orai1 interaction site (Feng et al., 2010) (Fig. 2). In the ΔN57 mutant three predicted short α helices are deleted, whereas the Orai1 interaction site remains present. The ΔN75 mutant disrupts the N-terminal Orai1 binding motif by removing critical residues V71 and T75. In the ΔN89 construct, only V95 of the Orai1 binding site remains, but the conserved helix-loop-helix motif in the N-terminus (residues 62–88) is now fully ablated. The shortest construct, ΔN101, has virtually no N-terminus and also V95 is now deleted. Since the C-terminus is just 20 amino acids long, only one truncation was made after TM10, ΔC927. Finally, a mutant with a combined truncation of the N- and C-termini, ΔN57/ΔC927, was generated.

According to immunoblotting (Fig. 3A) and fluorescence imaging (Fig. 3B), all GFP- or mCherry-labeled truncation mutants are well expressed above background. Compared to WT SPCA2, the subcellular localization of the truncation mutants in both HEK293T (Fig. 3B) and HeLa cells (Supplementary Fig. S1 in the online version at DOI: 10.1016/j.tice.2016.09.004) is different. In line with previous reports (Vanoevelen et al., 2005a), SPCA2 WT is localized in the perinuclear region demonstrating good overlap with the *trans*-Golgi marker TGN46 (Supplementary Fig. S1 in the online version at DOI: 10.1016/j.tice.2016.09.004) and little colocalization with SERCA2b (Fig. 3B), which corresponds to a Golgi localization. In contrast, all truncation mutants exhibit a distribution that overlaps mainly with SERCA2b (Fig. 3B) while little or no colocalization is observed with TGN46 (Supplementary Fig. S1 in the online version at DOI: 10.1016/j.tice.2016.09.004). This suggests that the truncation mutants occupy earlier compartments in the secretory pathway. Thus, the N- and C-termini might either determine

Please cite this article in press as: Smaardijk, S., et al., SPCA2 couples Ca^{2+} influx via Orai1 to Ca^{2+} uptake into the Golgi/secretory pathway. Tissue Cell (2016), http://dx.doi.org/10.1016/j.tice.2016.09.004

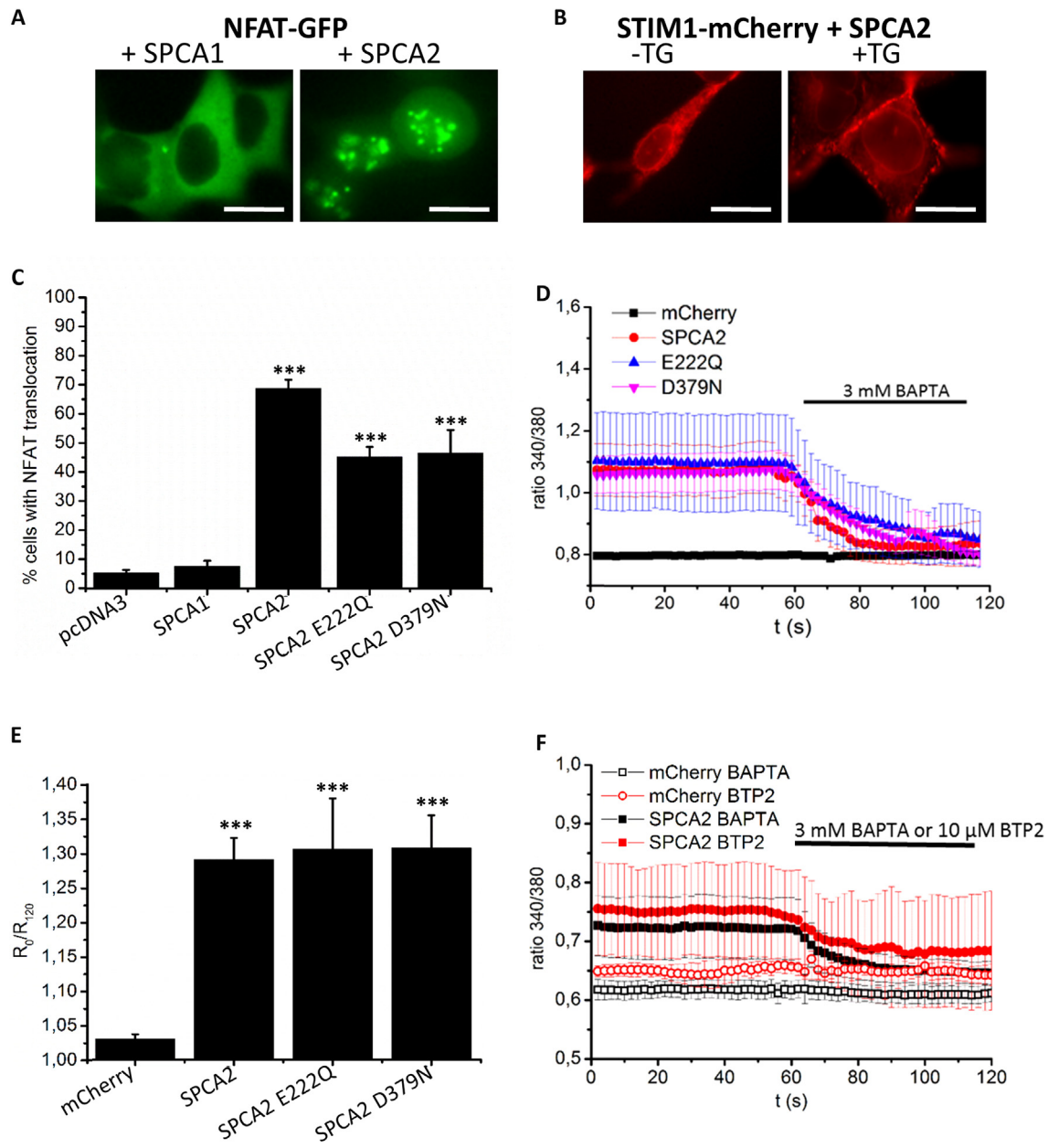

Fig. 1. SPCA2 overexpression increases $[Ca^{2+}]_{cyt}$ and constitutive Ca^{2+} influx. (A) Translocation of NFAT-GFP to the nucleus in HEK293T cells overexpressing SPCA1 or SPCA2. White Scale bar = 25 µm. (B) Relocalization of STIM1 into punctae is not induced by SPCA2 overexpression alone, but can be induced by addition of thapsigargin (TG), which reduces the $[Ca^{2+}]_{ER}$. (C) Quantification of the percentage of cells with NFAT nuclear translocation (n = 8, 100 cells per experiment were counted). (D) Fura2 340/380 ratios for HEK293T cells overexpressing mCherry or mCherry-tagged SPCA2 constructs. At the indicated time point, 3 mM BAPTA was added. (E) The constitutive Ca^{2+} influx mediated by SPCA2 and its inactive mutants was quantified by determining the R_0/R_{120} value, which is the starting 340/380 ratio at 0 s (R_0) normalized to the ratio after addition of BAPTA at 120 s (R_{120}). (F) Like the addition of 3 mM BAPTA, the inhibition of Orai1 with 10 µM BTP2 prevents SPCA2-mediated constitutive Ca^{2+} influx. Data are shown as average ± SEM. ***: $p < 0.005$. Fura2 data represent averages of 40–100 cells from at least four independent experiments.

the subcellular targeting of SPCA2 or alternatively, the truncation mutants might be unstable leading to retention in the ER. Of note, although we cannot exclude that the truncation mutants are present in the PM, no obvious PM localization was observed for either the WT or the mutants.

Despite the different subcellular localization, all N-terminal truncation mutants trigger a constitutive Ca^{2+} influx that is comparable to WT (Fig. 4A). In line with the critical role of the C-terminus in Orai1 activation (Feng et al., 2010), the R_0/R_{120} value of the ΔC927 mutant is not significantly different from the mCherry-control cells, but is significantly lower than WT, indicating that the Orai1 activation is prevented by the C-terminal deletion. Despite the predominant ER distribution of the N-terminal mutants and their capacity to induce Ca^{2+} influx, we excluded that SOCE is elicited as a consequence of ER stress, since STIM1-mCherry does not appear to relocalize into punctae (Fig. 3B).

Since the effect of all the N-terminal truncation mutants on Ca^{2+} influx is comparable, we further focused on the ΔN57 mutant, which is the most conservative N-terminal mutant with altered subcellular distribution, but intact SICE. We analyzed the impact of Orai1 knockdown on the constitutive Ca^{2+} influx over the PM. We first established that Orai1 knockdown completely abolished the ability of the cells to elicit a thapsigargin-dependent SOCE response (data not shown). Importantly, knockdown of Orai1 also prevented the constitutive Ca^{2+} influx induced by overexpression of WT or the ΔN57 truncation mutant (Fig. 4B). Together, our results sug-

Please cite this article in press as: Smaardijk, S., et al., SPCA2 couples Ca^{2+} influx via Orai1 to Ca^{2+} uptake into the Golgi/secretory pathway. Tissue Cell (2016), http://dx.doi.org/10.1016/j.tice.2016.09.004

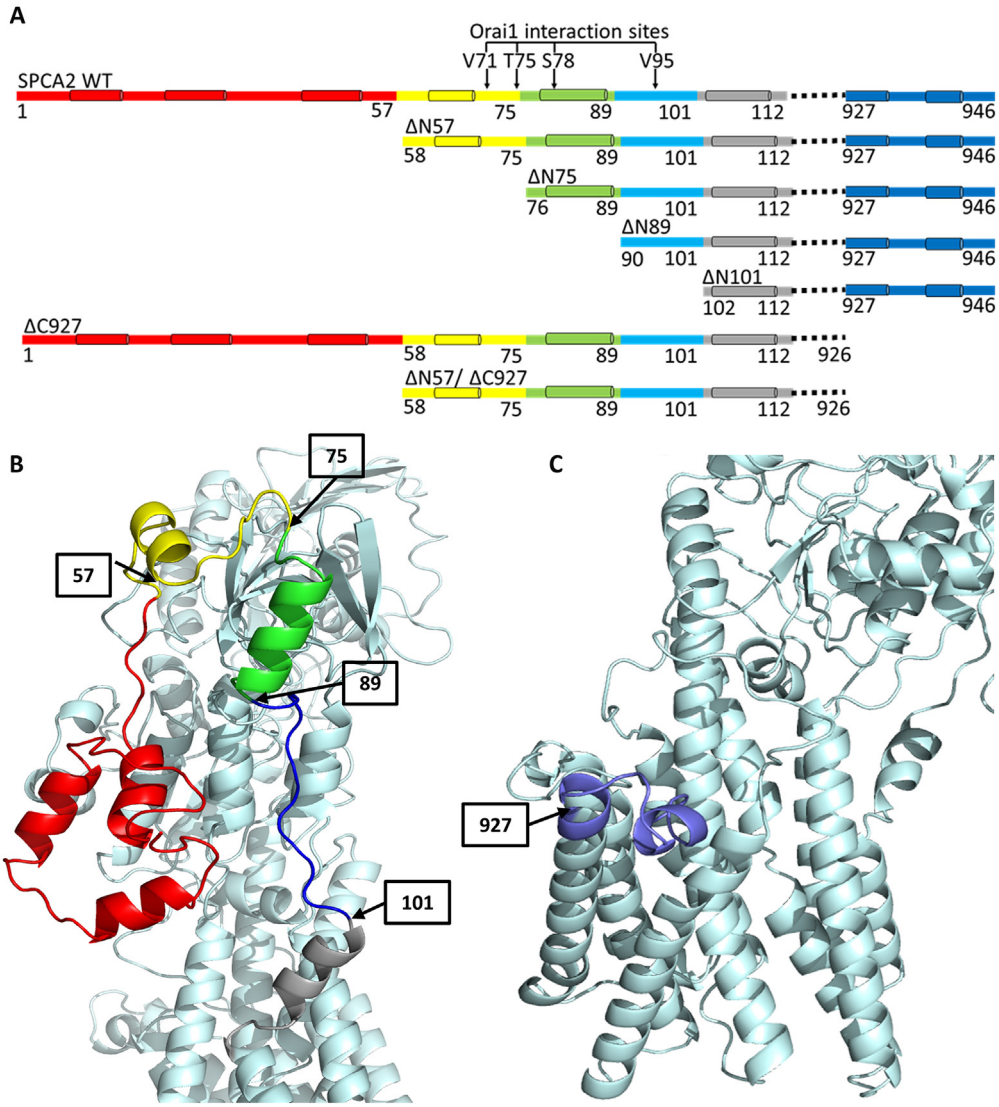

Fig. 2. Overview of the N- and C-terminal truncation mutants of SPCA2. (A) Schematic overview of the truncations depicting the residue numbers that were deleted based on the secondary structure prediction and the site of Orai1 interaction. On top, the predicted secondary structure of the SPCA2 N-terminus is highlighted (α-helices are represented by cylinders; no β-sheets are predicted), and the residues belonging to the Orai1 interaction site are indicated (Feng et al., 2010). (B–C) Homology model of SPCA2, with the N-terminal (B) or C-terminal (C) truncations indicated in the same colors as in (A). The SPCA2 homology model was generated with iTasser and is mainly based on structures of the closely related SERCA1a Ca^{2+} pump.

gest that the N-terminal truncation mutants evoke a SICE response via Orai1 while residing predominantly in earlier compartments of the secretory pathway.

3.3. *SPCA2 couples Orai1 mediated Ca^{2+} influx to Ca^{2+} uptake into the secretory pathway*

We therefore hypothesize that SPCA2 may activate Orai1 from an intracellular membrane instead of from within the PM as proposed by Feng et al. (2010), which might allow SPCA2 to directly shuttle the entering Ca^{2+} into the secretory pathway. To explore this, we evaluated the Ca^{2+} content in intracellular compartments upon overexpression of SPCA2. As assessed by thapsigargin treatment, overexpression of SPCA2 has little effect on ER Ca^{2+} levels, further supporting the conclusion that the SPCA2-mediated Ca^{2+} influx is SOCE-independent (Fig. 4C). However, subsequent ionomycin treatment shows that non-ER Ca^{2+} levels are dramatically increased, indicating that SICE is indeed coupled to uptake of Ca^{2+}, most likely into the Golgi/secretory pathway. This is further supported by the observation that ionomycin induced Ca^{2+} release is lowered by $46.6 \pm 1.9\%$ ($p < 0.05$) upon knockdown of Orai1 (Fig. 4D). In strong contrast, the truncation mutants ΔN57 and ΔC927 fail to increase the Ca^{2+} concentration in both the ER or non-ER stores (Fig. 4C), although Orai1 activation for the ΔN57 mutant was not impaired (Fig. 4A, B). The failure of the ΔN57 mutant to increase the intracellular Ca^{2+} store content might be explained by a loss of Ca^{2+} transport activity, since a similar pattern is observed with the inactive mutant E222Q (Fig. 4C). A combination of SPCA2 and Orai1 inactivation might explain why ΔC927 is unable to increase the intracellular Ca^{2+} store content.

To confirm the loss-of-transport activity of the ΔN57 and ΔC927 mutants, we compared the capacity of the mutants to auto-phosphorylate in response to Ca^{2+}, which is a hallmark of transport activity. To ensure detectable biochemical activity, we turned to the overexpression of unlabeled SPCA2 constructs in COS cells. Although WT SPCA2 is auto-phosphorylated in the presence of Ca^{2+}, the ΔN57 and ΔC927 mutants fail to undergo auto-phosphorylation (Fig. 4E). Note that we also observed a lower expression level of the ΔN57 mutant, which is likely explained by a reduced stability. Indeed, inhibition of the proteasome by

Please cite this article in press as: Smaardijk, S., et al., SPCA2 couples Ca^{2+} influx via Orai1 to Ca^{2+} uptake into the Golgi/secretory pathway. Tissue Cell (2016), http://dx.doi.org/10.1016/j.tice.2016.09.004

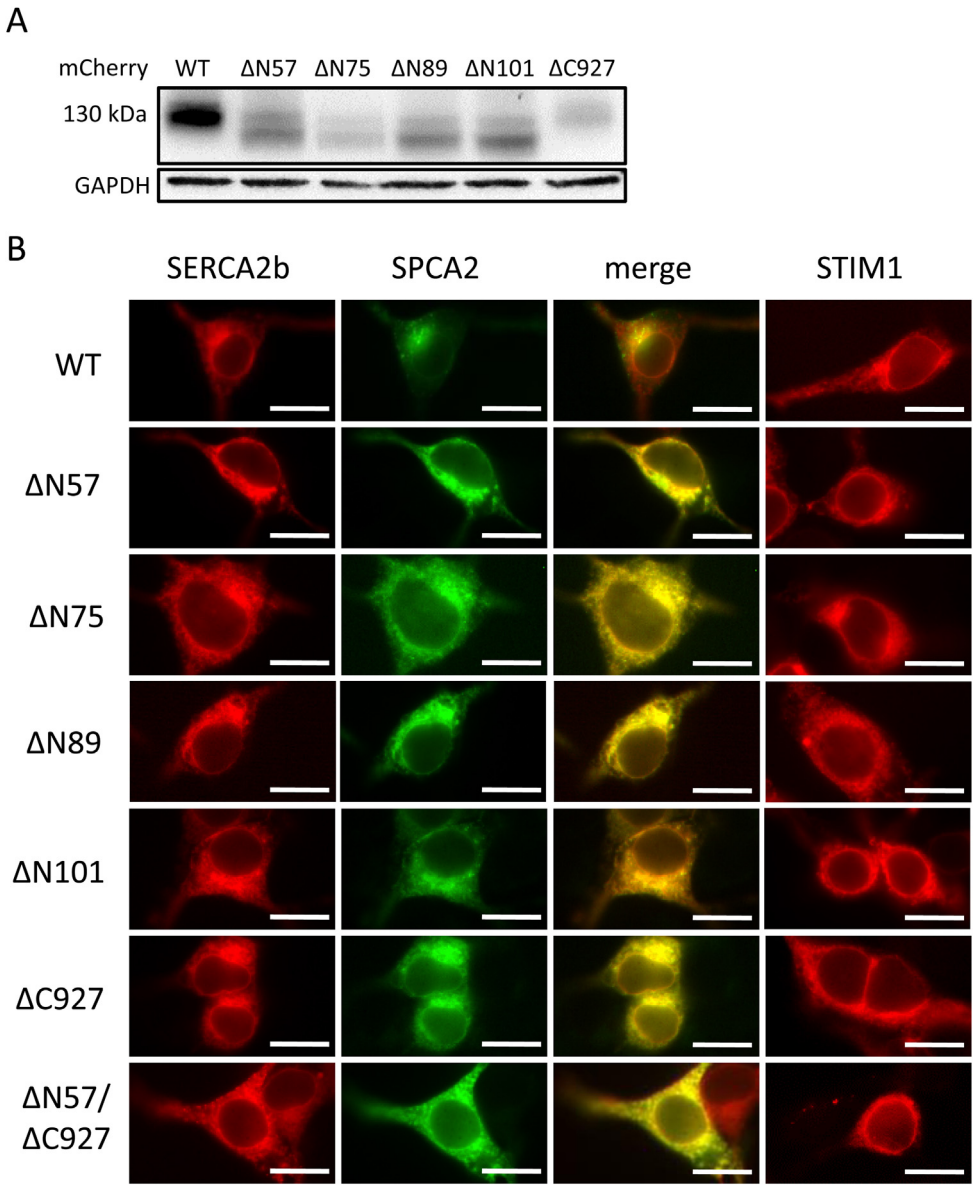

Fig. 3. SPCA2 truncation mutants localize predominantly to the ER. (A) Representative immunoblot with an mCherry-specific antibody displaying the relative expression levels of mCherry-tagged SPCA2 WT and truncation mutants in total membrane fractions of HEK293T cells. The immunoblot depicting the GAPDH levels serves as a loading control. (B) Representative fluorescence images of HEK293T cells overexpressing N-terminally GFP-labeled SPCA2 WT or truncation mutants and N-terminal labeled mCherry-SERCA2b or mCherry-STIM1. (n = 3) White scale bar: 25 μm.

MG-132 leads to comparable expression levels of the ΔN57 and WT/ΔC927 mutants (Fig. 4F). Noteworthy, addition of an N-terminal mCherry/GFP-tag leads to a partial stabilization of the protein (Fig. 3A). By combining the results of Fig. 4C and E, we conclude that the N- and C-termini are important for the SPCA2 transport activity, which mediates Ca^{2+} transfer into the Golgi/secretory pathway.

4. Discussion

4.1. The SPCA2 N- and C-termini control SICE and SPCA2 activity

The secretory pathway Ca^{2+} ATPase SPCA2 contributes to uptake of Ca^{2+} and Mn^{2+} in the Golgi/secretory pathway, but SPCA2 also triggers Orai1 activation in a process termed SICE, which seems to occur independent of STIM1/Orai1 activation. Here, we confirm previous findings that overexpression of SPCA2 mediates constitutive Ca^{2+} influx, leading to a rise of $[Ca^{2+}]_{cyt}$ and NFAT translocation into the nucleus (Feng et al., 2010). Like 2-APB and miconazole (Feng et al., 2010), the CRAC inhibitor BTP2 and Orai1 knockdown block the constitutive Ca^{2+} influx, further strengthening the conclusion that SICE depends on Orai1.

SICE also critically depends on the SPCA2 C-terminus. Although the SPCA2 C-terminus is short and relatively unstructured, we confirm that its removal inhibits SICE (Feng et al., 2010). Moreover, expression of a C-terminal fragment of SPCA2 that only includes transmembrane segments 9 and 10 (TM9-10) is sufficient to induce Orai1 activation (Feng et al., 2010). Now, we show that the C-terminus of SPCA2 also impacts on subcellular targeting and Ca^{2+} transport activity, further demonstrating its functional importance. The C-terminus of SPCA2 includes a putative PDZ-binding domain, which might be involved in Orai1 activation, membrane trafficking and regulation of Ca^{2+} uptake activity (Cross et al., 2013; Feng et al., 2010).

Thus, the C-terminus of SPCA2 activates Orai1, but interestingly this falls under the control of the SPCA2 N-terminus. A peptide

Please cite this article in press as: Smaardijk, S., et al., SPCA2 couples Ca^{2+} influx via Orai1 to Ca^{2+} uptake into the Golgi/secretory pathway. Tissue Cell (2016), http://dx.doi.org/10.1016/j.tice.2016.09.004

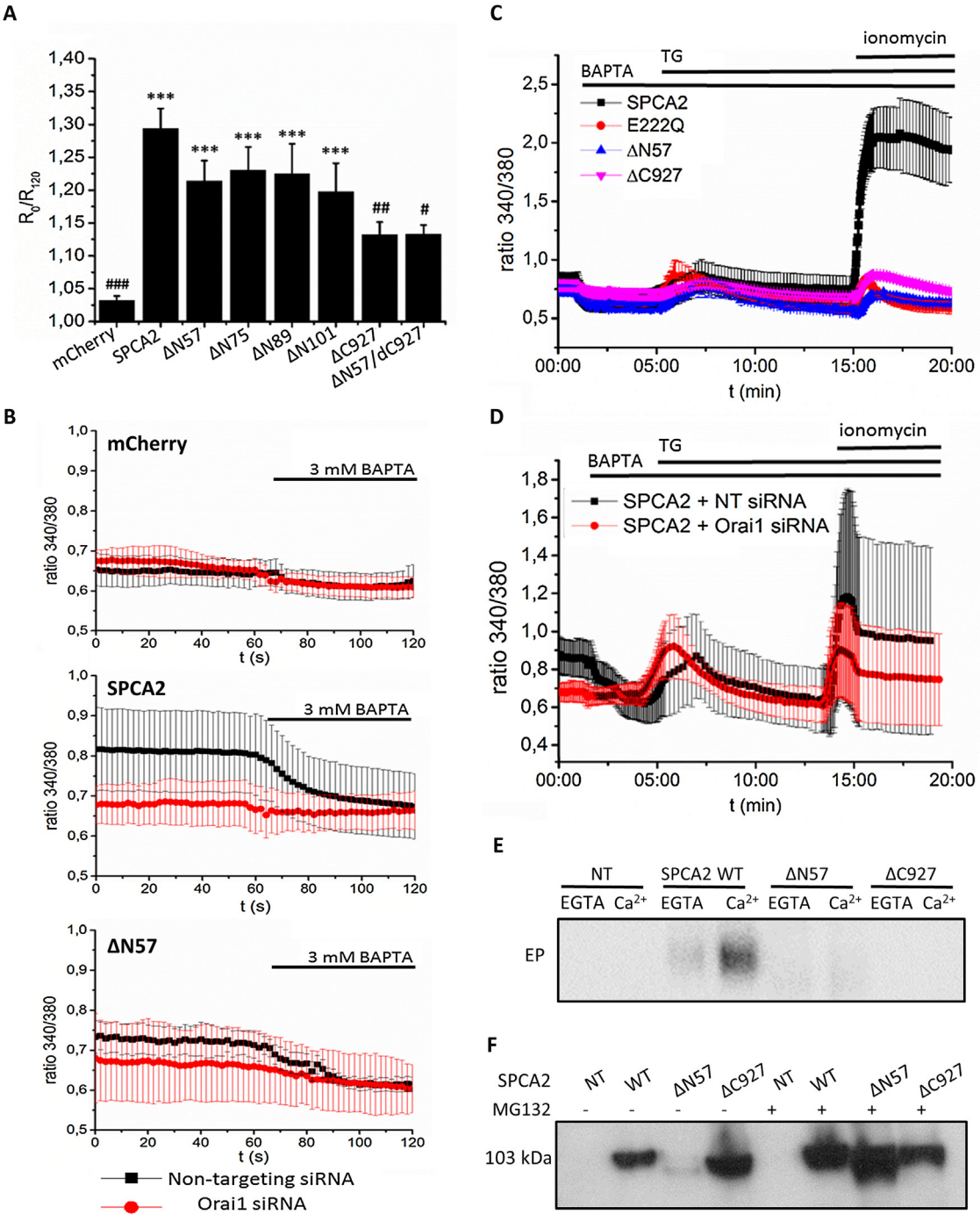

Fig. 4. N-/C-terminal truncations inactivate SPCA2 without affecting the capacity to elicit Orai1-dependent SICE. (A) The constitutive Ca^{2+} influx in HEK293T cells elicited by the overexpression of SPCA2 WT or N-/C-terminal truncation mutants was followed by Fura2 Ca^{2+} imaging. The bar graph represents the quantification of the constitutive Ca^{2+} influx, which is presented as the R_0/R_{120} value, i.e. the starting 340/380 Fura2 ratio at 0 s (R_0) normalized to the Fura2 ratio after addition of BAPTA at 120 s (R_{120}). Values are represented as average ± SEM. *, significant difference compared to mCherry. #, significant difference compared to SPCA2. One mark, $p < 0.05$; two marks, $p < 0.01$; three marks: $p < 0.005$. (B) Fura2 340/380 ratios of HEK293T cells cotransfected with mCherry or mCherry-tagged SPCA2 constructs and non-targeting or Orai1 siRNA. To block Ca^{2+} entry 3 mM BAPTA was added at the indicated time point. Values are represented as average ± SD. Result of a representative experiment is shown (n = 3, 10 cells tested per condition). (C) Fura2 340/380 ratios for HEK293T cells overexpressing SPCA2 WT, the inactive E222Q mutant or ΔN57 and ΔC927 truncation mutants. Addition of 3 mM BAPTA, 500 nM thapsigargin (TG) or 2 μM ionomycin is indicated. Values are represented as average ± SEM, and represent averages of 30–100 cells from at least three independent experiments. (D) Fura2 340/380 ratios of HEK293T cells overexpressing mCherry or mCherry-tagged SPCA2 constructs, cotransfected with non-targeting or Orai1 siRNA. Values are represented as average ± SD. Result of a representative experiment is shown (n = 2, 10 cells tested per condition). (E) Representative radiogram of a Ca^{2+}-dependent auto-phosphorylation assay showing the relative auto-phosphorylation of SPCA2 in total membrane fractions of COS cells overexpressing SPCA2 WT, ΔN57 and ΔC927 truncation mutants (n = 3). Total membrane fractions of non-transfected cells (NT) are provided as negative control. The auto-phosphorylation assay was conducted in the presence (100 μM $CaCl_2$) and absence (1 mM EGTA) of Ca^{2+}. (F) Representative immunoblot displaying relative expression levels of SPCA2 WT and ΔN57 and ΔC927 truncation mutants before and after treatment with 10 μM MG132 to inhibit protein degradation by the proteasome (n = 4).

Please cite this article in press as: Smaardijk, S., et al., SPCA2 couples Ca^{2+} influx via Orai1 to Ca^{2+} uptake into the Golgi/secretory pathway. Tissue Cell (2016), http://dx.doi.org/10.1016/j.tice.2016.09.004

stretch corresponding to the first 106 N-terminal residues of SPCA2 exerts a dominant negative effect on the SPCA2 C-terminal dependent NFAT translocation (Feng et al., 2010). Here, we demonstrate that truncations of the N-terminus abolish the negative control of the N-terminus on Orai1 activation by the SPCA2 C-terminus. We hypothesize that similar to the TM9-10 construct (Feng et al., 2010), removal of (parts of) the N-terminus leads to a permanent exposure of the SPCA2 C-terminus, which might explain the constitutive Orai1 activation. Thus, our results confirm that the SPCA2 C-terminus is required for Orai1 activation, but that the N-terminus is dispensable, merely serving as a regulator of the C-terminus. Based on our truncation experiments, the SPCA2 segment that is responsible for the regulation of the C-terminal-mediated activation of Orai1 is most likely found within the first 57 amino acids of SPCA2.

Besides a regulatory effect on the C-terminus for inducing SICE, we demonstrate that the N-terminus is also important for Ca^{2+} transport activity, stability and intracellular targeting. We show that the N-terminal truncation mutant ΔN57 is inactive, demonstrating the importance of the N-terminus for SPCA2 activity. We cannot fully rule out that the inactivity of the N-terminal mutant might (at least in part) relate to instability and improper folding, but despite this, ΔN57 (and other N-terminal truncation mutants) triggers SICE. A role of the N-terminus in controlling the SPCA2 activity is in line with a previous report on the yeast orthologue PMR1. N-terminal mutations in PMR1, notably at the corresponding position of the putative Orai1 interaction site in SPCA2, lead to defective Ca^{2+} transport and/or altered ion specificity (Wei et al., 1999).

The importance of the SPCA2 N-terminus for regulating Orai1 activation and SPCA2 activity, suggests that the N-terminus may control the C-terminus by intramolecular interactions. Ca^{2+} pumps undergo dramatic conformational changes in the transport cycle (Moller et al., 2005; Vangheluwe et al., 2009), possibly affecting the intramolecular interactions of the N- and C-termini on SPCA2. We tested this by comparing the E1 (D379N) or E2P (E222Q) mutants, but we observed that both mutants behave similar to WT in their capacity to elicit SICE. However, the E222Q mutant may not be exclusively trapped in the predicted E2P conformation (Clausen et al., 2013) or other major SPCA2 conformations (E2, E1P) may show a different effect on the Orai1 activation.

4.2. SPCA2 couples Ca^{2+} influx via Orai1 to Ca^{2+} uptake in the Golgi/secretory pathway

We confirm previous observations on the D379N mutant that SPCA2 activity is not required for Orai1 activation (Feng et al., 2010), and extend these observations to at least two other inactive SPCA2 mutants (E222Q and ΔN57). The capacity of these mutants to induce SICE remains intact, while SPCA2 transport activity is impaired, indicating that it is possible to uncouple SICE and SPCA2 activity. However, this does not exclude the possibility that in physiological conditions the Orai1 activation and SPCA2 transport function might be tightly connected. In fact, our results suggest that the SPCA2 N-/C-termini regulate both Orai1 activation and SPCA2 activity. In addition, we show that SPCA2-mediated Ca^{2+} influx via Orai1 is efficiently coupled to SPCA2-mediated uptake of Ca^{2+}, most likely into the Golgi/secretory pathway where SPCA2 is present. We also demonstrate that Orai1 knockdown not only reduces the SPCA2-mediated rise in cytosolic Ca^{2+} concentration, but also significantly diminishes the intracellular Ca^{2+} store content.

Feng et al. proposed that the SPCA2/Orai1 activation takes place within the PM (Feng et al., 2010), but efficient Ca^{2+} transfer into the Golgi and secretory pathway probably depends on an active SPCA2 pump present in intracellular membranes. It is therefore equally possible that SPCA2 might directly interact with and activate Orai1 from an intracellular membrane that is in close proximity to the PM. In mouse mammary epithelial cells the SPCA2 C-terminus promotes the trafficking of Orai1 towards the PM, suggesting that Orai1 and SPCA2 may already interact in earlier compartments in the secretory route (Cross et al., 2013). Moreover, according to our imaging experiments little SPCA2 is present in the PM, whereas the majority of SPCA2 is localized in intracellular membranes where Ca^{2+} uptake is stimulated. The N-terminal truncation mutants are still able to activate Orai1 while residing predominantly in the ER, suggesting that the SPCA2/Orai1 interaction may also take place from an intracellular compartment earlier in the secretory pathway (Cross et al., 2013).

Contact sites between the Golgi and PM are not yet described, but SPCA2 might interact with Orai1 from various intracellular membranes, such as sub-compartments of the Golgi apparatus, secretory vesicles and/or ER. In comparison, the STIM1/Orai1 interaction is a well-studied example of a contact between the ER and the PM, which is formed in conditions of ER Ca^{2+} depletion (Zhang et al., 2005). The activation of this complex ensures refilling of the ER indirectly via the SERCA Ca^{2+} pumps. In analogy, we propose that in secretory cells, efficient Ca^{2+} filling of the Golgi or Golgi-derived vesicles may depend on the SPCA2 Ca^{2+} pump that works together with the Orai1 Ca^{2+} channel in a micro-domain near the PM. Of interest, the subcellular localization of SPCA2 varies between cell types (Cross et al., 2013; Vanoevelen et al., 2005a,b; Xiang et al., 2005), suggesting that the intracellular membranes where the SPCA2/Orai1 complex is formed might be cell type dependent.

4.3. Implications for lactation and breast cancer

In lactating mammary gland cells, the expression of SPCA2 and Orai1, but not STIM1/2, is coordinately upregulated (McAndrew et al., 2011). Orai1 is predominantly found in the basolateral membrane where it enables Ca^{2+} influx from the blood into the mammary cells (Cross et al., 2013). SPCA2 is mainly located in extra-Golgi vesicles of lactating mammary tissue and mammospheres, but in mammospheres SPCA2 punctae are observed immediately underneath the PM in close, but not overlapping position with Orai1 (Cross et al., 2013). This localization might be in line with a model of Orai1 activation by SPCA2 from sub-PM Golgi-derived vesicles. Whether SPCA2 could interact with Orai1 from a sub-PM compartment remains to be further established, but a direct physical or merely functional coupling between Orai1 in the PM and SPCA2 in the Golgi/secretory vesicles may shuttle Ca^{2+} from the extracellular environment into the secretory system for subsequent delivery into milk. Moreover, SPCA2 may chronically interact with Orai1 in breast cancer. This results in an increased proliferation of MCF-7 cells and growth in soft agar, which can be counteracted by SPCA2 or Orai1 knockdown. Thus, targeting the SPCA2/Orai1 complex might be of therapeutic interest in breast cancer (Feng et al., 2010).

In conclusion, SPCA2 elicits Ca^{2+} influx via store independent activation of Orai1 and subsequently promotes uptake of Ca^{2+} into intracellular compartments, a process that is tightly controlled by the SPCA2 N- and C-termini. This coordinated action of an intracellular Ca^{2+} pump and a PM Ca^{2+} channel might be of physiological importance to shuttle Ca^{2+} into the secretory pathway of secreting cells, such as mammary gland during lactation.

Acknowledgements

This work has been funded by the Flanders Research Foundation FWO (G044212N and G0B1115N) and the Inter-University Attraction Poles program (P7/13). We thank Dr. J. Vanoevelen for providing help and support at the start of the project.

Please cite this article in press as: Smaardijk, S., et al., SPCA2 couples Ca^{2+} influx via Orai1 to Ca^{2+} uptake into the Golgi/secretory pathway. Tissue Cell (2016), http://dx.doi.org/10.1016/j.tice.2016.09.004

References

Baron, S., Vangheluwe, P., Sepulveda, M.R., Wuytack, F., Raeymaekers, L., Vanoevelen, J., 2010. The secretory pathway Ca(2+)-ATPase 1 is associated with cholesterol-rich microdomains of human colon adenocarcinoma cells. Biochim. Biophys. Acta 1798, 1512–1521.

Berridge, M.J., Bootman, M.D., Roderick, H.L., 2003. Calcium signalling: dynamics, homeostasis and remodelling. Nat. Rev. Mol. Cell Biol. 4, 517–529.

Clausen, J.D., Bublitz, M., Arnou, B., Montigny, C., Jaxel, C., Moller, J.V., Nissen, P., Andersen, J.P., le Maire, M., 2013. SERCA mutant E309Q binds two Ca(2+) ions but adopts a catalytically incompetent conformation. EMBO J. 32, 3231–3243.

Cross, B.M., Hack, A., Reinhardt, T.A., Rao, R., 2013. SPCA2 regulates orai1 trafficking and store independent Ca(2 +) entry in a model of lactation. PLoS One 8, e67348.

Dang, D., Rao, R., 2016. Calcium-ATPases: gene disorders and dysregulation in cancer. Biochim. Biophys. Acta 1863, 1344–1350.

Durr, G., Strayle, J., Plemper, R., Elbs, S., Klee, S.K., Catty, P., Wolf, D.H., Rudolph, H.K., 1998. The medial-Golgi ion pump Pmr1 supplies the yeast secretory pathway with Ca2+ and Mn2+ required for glycosylation, sorting, and endoplasmic reticulum-associated protein degradation. Mol. Biol. Cell 9, 1149–1162.

Faddy, H.M., Smart, C.E., Xu, R., Lee, G.Y., Kenny, P.A., Feng, M., Rao, R., Brown, M.A., Bissell, M.J., Roberts-Thomson, S.J., Monteith, G.R., 2008. Localization of plasma membrane and secretory calcium pumps in the mammary gland. Biochem. Biophys. Res. Commun. 369, 977–981.

Falchetto, R., Vorherr, T., Carafoli, E., 1992. The calmodulin-binding site of the plasma membrane Ca2+ pump interacts with the transduction domain of the enzyme. Protein Sci. 1, 1613–1621.

Feng, M., Grice, D.M., Faddy, H.M., Nguyen, N., Leitch, S., Wang, Y., Muend, S., Kenny, P.A., Sukumar, S., Roberts-Thomson, S.J., Monteith, G.R., Rao, R., 2010. Store-independent activation of Orai1 by SPCA2 in mammary tumors. Cell 143, 84–98.

Gorski, P.A., Trieber, C.A., Lariviere, E., Schuermans, M., Wuytack, F., Young, H.S., Vangheluwe, P., 2012. Transmembrane helix 11 is a genuine regulator of the endoplasmic reticulum Ca2+ pump and acts as a functional parallel of beta-subunit on alpha-Na+,K+-ATPase. J. Biol. Chem. 287, 19876–19885.

Grice, D.M., Vetter, I., Faddy, H.M., Kenny, P.A., Roberts-Thomson, S.J., Monteith, G.R., 2010. Golgi calcium pump secretory pathway calcium ATPase 1 (SPCA1) is a key regulator of insulin-like growth factor receptor (IGF1R) processing in the basal-like breast cancer cell line MDA-MB-231. J. Biol. Chem. 285, 37458–37466.

Hogan, P.G., Chen, L., Nardone, J., Rao, A., 2003. Transcriptional regulation by calcium, calcineurin, and NFAT. Genes Dev. 17, 2205–2232.

Holemans, T., Sorensen, D.M., van Veen, S., Martin, S., Hermans, D., Kemmer, G.C., Van den Haute, C., Baekelandt, V., Gunther Pomorski, T., Agostinis, P., Wuytack, F., Palmgren, M., Eggermont, J., Vangheluwe, P., 2015. A lipid switch unlocks Parkinson's disease-associated ATP13A2. Proc. Natl. Acad. Sci. U. S. A. 112, 9040–9045.

Kienzle, C., Basnet, N., Crevenna, A.H., Beck, G., Habermann, B., Mizuno, N., von Blume, J., 2014. Cofilin recruits F-actin to SPCA1 and promotes Ca2+-mediated secretory cargo sorting. J. Cell Biol. 206, 635–654.

Leitch, S., Feng, M., Muend, S., Braiterman, L.T., Hubbard, A.L., Rao, R., 2011. Vesicular distribution of secretory pathway Ca^{2+}-ATPase isoform 1 and a role in manganese detoxification in liver-derived polarized cells. Biometals 24, 159–170.

McAndrew, D., Grice, D.M., Peters, A.A., Davis, F.M., Stewart, T., Rice, M., Smart, C.E., Brown, M.A., Kenny, P.A., Roberts-Thomson, S.J., Monteith, G.R., 2011. ORAI1-mediated calcium influx in lactation and in breast cancer. Mol. Cancer Ther. 10, 448–460.

Moller, J.V., Nissen, P., Sorensen, T.L., le Maire, M., 2005. Transport mechanism of the sarcoplasmic reticulum Ca2+ −ATPase pump. Curr. Opin. Struct. Biol. 15, 387–393.

Okunade, G.W., Miller, M.L., Azhar, M., Andringa, A., Sanford, L.P., Doetschman, T., Prasad, V., Shull, G.E., 2007. Loss of the Atp2c1 secretory pathway Ca^{2+}-ATPase (SPCA1) in mice causes Golgi stress, apoptosis, and midgestational death in homozygous embryos and squamous cell tumors in adult heterozygotes. J. Biol. Chem. 282, 26517–26527.

Park, C.Y., Hoover, P.J., Mullins, F.M., Bachhawat, P., Covington, E.D., Raunser, S., Walz, T., Garcia, K.C., Dolmetsch, R.E., Lewis, R.S., 2009. STIM1 clusters and activates CRAC channels via direct binding of a cytosolic domain to Orai1. Cell 136, 876–890.

Pizzo, P., Lissandron, V., Pozzan, T., 2010. The trans-golgi compartment: a new distinct intracellular Ca store. Commun. Integr. Biol. 3, 462–464.

Pizzo, P., Lissandron, V., Capitanio, P., Pozzan, T., 2011. Ca(2+) signalling in the Golgi apparatus. Cell Calcium 50, 184–192.

Reinhardt, T.A., Filoteo, A.G., Penniston, J.T., Horst, R.L., 2000. Ca(2+)-ATPase protein expression in mammary tissue. Am. J. Physiol. Cell Physiol. 279, C1595–C1602.

Reinhardt, T.A., Lippolis, J.D., Shull, G.E., Horst, R.L., 2004. Null mutation in the gene encoding plasma membrane Ca2+-ATPase isoform 2 impairs calcium transport into milk. J. Biol. Chem. 279, 42369–42373.

Rizzuto, R., Pozzan, T., 2006. Microdomains of intracellular Ca2+: molecular determinants and functional consequences. Physiol. Rev. 86, 369–408.

Sepúlveda, M.R., Marcos, D., Berrocal, M., Raeymaekers, L., Mata, A.M., Wuytack, F., 2008. Activity and localization of the secretory pathway Ca2+-ATPase isoform 1 (SPCA1) in different areas of the mouse brain during postnatal development. Mol. Cell. Neurosci. 38, 461–473.

Sudbrak, R., Brown, J., Dobson-Stone, C., Carter, S., Ramser, J., White, J., Healy, E., Dissanayake, M., Larrègue, M., Perrussel, M., Lehrach, H., Munro, C.S., Strachan, T., Burge, S., Hovnanian, A., Monaco, A.P., 2000. Hailey–Hailey disease is caused by mutations in ATP2C1 encoding a novel Ca^{2+} pump. Hum. Mol. Genet. 9, 1131–1140.

Vandecaetsbeek, I., Trekels, M., De Maeyer, M., Ceulemans, H., Lescrinier, E., Raeymaekers, L., Wuytack, F., Vangheluwe, P., 2009. Structural basis for the high Ca2+ affinity of the ubiquitous SERCA2b Ca2+ pump. Proc. Natl. Acad. Sci. U. S. A. 106, 18533–18538.

Vangheluwe, P., Sepúlveda, M.R., Missiaen, L., Raeymaekers, L., Wuytack, F., Vanoevelen, J., 2009. Intracellular Ca^{2+}- and Mn^{2+}-transport ATPases. Chem. Rev. 109, 4733–4759.

Vanoevelen, J., Dode, L., Van Baelen, K., Fairclough, R.J., Missiaen, L., Raeymaekers, L., Wuytack, F., 2005a. The secretory pathway Ca^{2+}/Mn^{2+}-ATPase 2 is a Golgi-localized pump with high affinity for Ca^{2+} ions. J. Biol. Chem. 280, 22800–22808.

Vanoevelen, J., Raeymaekers, L., Dode, L., Parys, J.B., De Smedt, H., Callewaert, G., Wuytack, F., Missiaen, L., 2005b. Cytosolic Ca2+ signals depending on the functional state of the Golgi in HeLa cells. Cell Calcium 38, 489–495.

Vervliet, T., Decrock, E., Molgo, J., Sorrentino, V., Missiaen, L., Leybaert, L., De Smedt, H., Kasri, N.N., Parys, J.B., Bultynck, G., 2014. Bcl-2 binds to and inhibits ryanodine receptors. J. Cell Sci. 127, 2782–2792.

Wei, Y., Marchi, V., Wang, R., Rao, R., 1999. An N-terminal EF hand-like motif modulates ion transport by Pmr1, the yeast Golgi Ca^{2+}/Mn^{2+}-ATPase. Biochemistry 38, 14534–14541.

Wong, A.K., Capitanio, P., Lissandron, V., Bortolozzi, M., Pozzan, T., Pizzo, P., 2013. Heterogeneity of Ca2+ handling among and within Golgi compartments. J. Mol. Cell Biol. 5, 266–276.

Xiang, M., Mohamalawari, D., Rao, R., 2005. A novel isoform of the secretory pathway Ca2+,Mn(2+)-ATPase, hSPCA2, has unusual properties and is expressed in the brain. J. Biol. Chem. 280, 11608–11614.

Zhang, S.L., Yu, Y., Roos, J., Kozak, J.A., Deerinck, T.J., Ellisman, M.H., Stauderman, K.A., Cahalan, M.D., 2005. STIM1 is a Ca2+ sensor that activates CRAC channels and migrates from the Ca2+ store to the plasma membrane. Nature 437, 902–905.

Zhang, Y., 2008. I-TASSER server for protein 3D structure prediction. BMC Bioinform. 9, 40.

Zitt, C., Strauss, B., Schwarz, E.C., Spaeth, N., Rast, G., Hatzelmann, A., Hoth, M., 2004. Potent inhibition of Ca2+ release-activated Ca2+ channels and T-lymphocyte activation by the pyrazole derivative BTP2. J. Biol. Chem. 279, 12427–12437.

von Blume, J., Alleaume, A.M., Cantero-Recasens, G., Curwin, A., Carreras-Sureda, A., Zimmermann, T., van Galen, J., Wakana, Y., Valverde, M.A., Malhotra, V., 2011. ADF/cofilin regulates secretory cargo sorting at the TGN via the Ca2+ ATPase SPCA1. Dev. Cell 20, 652–662.

Please cite this article in press as: Smaardijk, S., et al., SPCA2 couples Ca^{2+} influx via Orai1 to Ca^{2+} uptake into the Golgi/secretory pathway. Tissue Cell (2016), http://dx.doi.org/10.1016/j.tice.2016.09.004